THE NASA AIRBORNE TROPICAL TROPOPAUSE EXPERIMENT

High-Altitude Aircraft Measurements in the Tropical Western Pacific

Eric J. Jensen, Leonhard Pfister, David E. Jordan, Thaopaul V. Bui, Rei Ueyama, Hanwant B. Singh, Troy D. Thornberry, Andrew W. Rollins, Ru-Shan Gao, David W. Fahey, Karen H. Rosenlof, James W. Elkins, Glenn S. Diskin, Joshua P. DiGangi, R. Paul Lawson, Sarah Woods, Elliot L. Atlas, Maria A. Navarro Rodriguez, Steven C. Wofsy, Jasna Pittman, Charles G. Bardeen, Owen B. Toon, Bruce C. Kindel, Paul A. Newman, Matthew J. McGill, Dennis L. Hlavka, Leslie R. Lait, Mark R. Schoeberl, John W. Bergman, Henry B. Selkirk, M. Joan Alexander, Ji-Eun Kim, Boon H. Lim, Jochen Stutz, and Klaus Pfeilsticker

We describe the Global Hawk flights and the measurements made during the NASA Airborne Tropical Tropopause Experiment (ATTREX) 2014 western Pacific campaign based in Guam.

The National Aeronautics and Space Administration (NASA) Airborne Tropical Tropopause Experiment (ATTREX) was a 5-yr airborne science program focused on the physical processes occurring in the tropical tropopause layer (TTL; ≃13–19 km). Inasmuch as the Brewer–Dobson circulation transports air upward through the TTL and then throughout the entire stratosphere, processes controlling TTL composition provide a boundary condition for stratospheric composition. A particular focus of ATTREX is the dehydration of air entering the stratosphere by ice crystal growth and sedimentation near the cold tropical tropopause. Radiative transfer calculations show that even small changes in stratospheric humidity have climate impacts that are significant compared to those of decadal increases in greenhouse gases (Forster and Shine 2002; Solomon et al. 2010). While the tropospheric water vapor–climate feedback is well represented in global models, predictions of future changes in stratospheric humidity are highly uncertain because of gaps in our understanding of physical processes occurring in the TTL. Uncertainties in the TTL transport processes and chemical composition also limit our ability to predict future changes in stratospheric ozone. The 2014 ATTREX deployment to Guam was particularly valuable for addressing these science issues given that the lowest tropopause temperatures, driest TTL air, and strongest upward transport occur in the western Pacific during boreal wintertime.

Stratospheric humidity and chemical composition are controlled by a complex interplay of processes occurring in the TTL (Fig. 1). Deep convection links surface conditions to the upper troposphere. The strength and depth of convection impacts transport of water vapor and chemical constituents to the TTL,

and deep convection is the predominant source of tropical waves. Tropical waves affect TTL thermal structure cirrus formation, and wave breaking and dissipation in the stratosphere drive large-scale ascent in the tropics. Ubiquitous TTL cirrus have a direct effect on Earth's radiation budget, and their regulation of stratospheric humidity results in an indirect radiative effect. TTL processes also influence the stratospheric ozone layer. Since precursors of ozone-depleting substances pass through the TTL before reaching the stratosphere, the TTL composition has a controlling influence on rates of stratospheric ozone destruction (Fueglistaler et al. 2009).

The ATTREX project used the long-range (16,000 km), high-altitude (20 km) NASA Global Hawk unmanned aircraft system for TTL measurements (Fig. 2). The ATTREX Global Hawk payload consisted of 12 instruments measuring cloud properties, water vapor, meteorological conditions, chemical tracers, chemical radicals, and radiation (see Table 1). The overall ATTREX project was managed by the NASA Ames Research Center (ARC), and the Global Hawk program is managed by Armstrong Flight Research Center (AFRC, formerly Dryden Flight Research Center). Prior to the Guam deployment, two ATTREX flight series were conducted out of AFRC, providing measurements in the central and eastern Pacific TTL [see Jensen et al. (2013b) for details]. We report here on the January–March 2014 ATTREX deployment to Guam (13°28′0″N, 144°46′59″E), which provided measurements in the western Pacific.

ATTREX GLOBAL HAWK PAYLOAD. The ATTREX payload was designed to address key uncertainties in our understanding of TTL composition, transport, and cloud processes affecting water vapor and short-lived trace gases. Measurements of water vapor, cloud properties, numerous chemical tracers, key radical species, meteorological conditions, and radiative fluxes were included (Table 1). Instruments were chosen based on proven techniques and size/weight accommodation on the Global Hawk.

The very dry conditions present in the tropical tropopause region (H_2O mixing ratios as low as ≃1 ppmv) represent a significant challenge for accurately measuring water vapor. Large, unresolved discrepancies between past water vapor concentrations measured with different instruments (Oltmans and Rosenlof 2000; Weinstock et al. 2009) have generally precluded the use of the measurements for detailed studies of cloud microphysical processes.

The water vapor measurement challenges were addressed in ATTREX by including two complementary instruments, namely, a diode laser hygrometer (DLH) and National Oceanic and Atmospheric Administration (NOAA) Water (NW), both of which have suitable sensitivity for measuring water vapor values as low as 1 ppmv. The NW instrument (added to the payload in 2013) provides a closed-cell tunable-diode laser (TDL) measurement that includes the in-flight calibration system used on the NOAA chemical ionization mass spectrometer (CIMS) instrument during the Middle Latitude Airborne Cirrus Properties Experiment (MACPEX; Thornberry et al. 2015). Calibration during the flights avoids the uncertainty associated with assuming that ground-based calibrations apply to in-flight conditions. The NW instrument also measures total water concentration using a forward-facing inlet that enhances ice concentration. The DLH instrument provides an open-path TDL measurement by firing the laser from the fuselage to a reflector on the wing and measuring the return

AFFILIATIONS: Jensen, Pfister, Jordan, Bui, Ueyama, and Singh—NASA Ames Research Center, Moffett Field, California; Thornberry and Rollins—NOAA/Earth System Research Laboratory, and Cooperative Institute for Research in Environmental Sciences, Boulder, Colorado; Gao, Fahey, Rosenlof, and Elkins—NOAA/Earth System Research Laboratory, Boulder, Colorado; Diskin and DiGangi—NASA Langley Research Center, Hampton, Virginia; Lawson and Woods—SPEC Inc., Boulder, Colorado; Atlas and Navarro Rodriguez—University of Miami, Miami, Florida; Wofsy and Pittman—Harvard University, Cambridge, Massachusetts; Bardeen—National Center for Atmospheric Research, Boulder, Colorado; Toon and Kindel—University of Colorado Boulder, Boulder, Colorado; Newman and McGill—NASA Goddard Space Flight Center, Greenbelt, Maryland; Hlavka—Science Systems and Applications, Inc., Greenbelt, Maryland; Lait—Morgan State University, Baltimore, Maryland; Schoeberl—Science and Technology Corporation, Columbia, Maryland; Bergman—Bay Area Environmental Research Institute, Sonoma, California; Selkirk—University Space Research Associates, Greenbelt, Maryland; Alexander and Kim—North-West Research Associates, Colorado Research Associates Office, Boulder, Colorado; Lim—Jet Propulsion Laboratory, Pasadena, California; Stutz—University of California, Los Angeles, Los Angeles, California; Pfeilsticker—University of Heidelberg, Heidelberg, Germany
CORRESPONDING AUTHOR E-MAIL: Eric J. Jensen, eric.j.jensen@nasa.gov

The abstract for this article can be found in this issue, following the table of contents.
DOI:10.1175/BAMS-D-14-00263.1

In final form 3 December 2015

signal. The pathlength (12.2 m) is long enough to provide a precise, fast measurement of water vapor. The precision is sufficient to permit detection of fine structure in the TTL water vapor field even at a data rate approaching 100 Hz. With typical flight speeds of 170 m s^{-1} and ascent/descent rates of 10 m s^{-1}, DLH provides measurements with spatial resolution determined by the geometry of its optical path: about 6 m horizontally and less than 0.5 m vertically. Temperature, pressure, and wind measurements were made with the Meteorological Measurement System (MMS) that also provided high-frequency data (up to 20 Hz) and permits examinations of fine structures in the relative humidity field and their correlation with cloud variations (Jensen et al. 2013a).

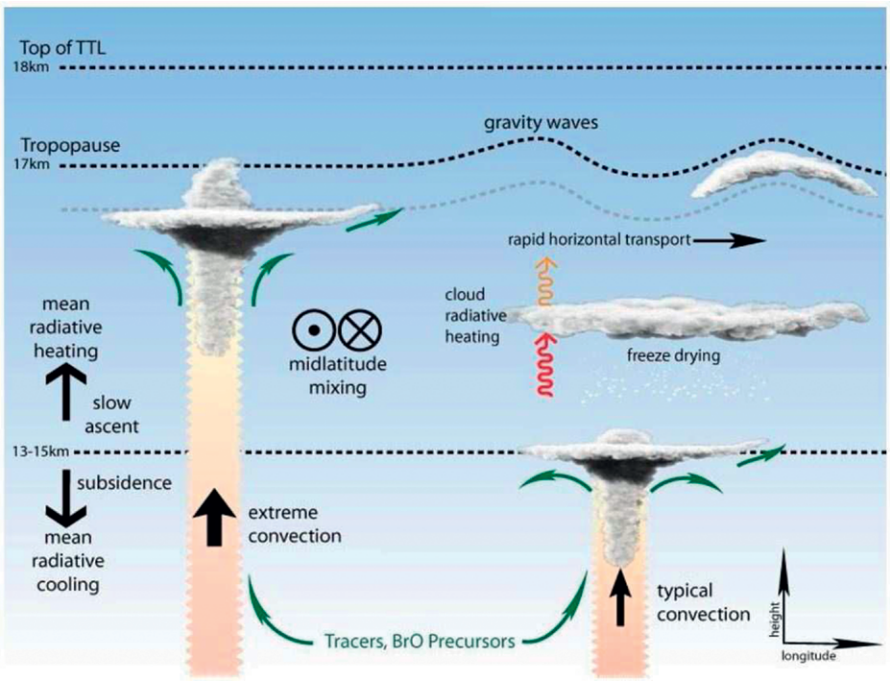

Fig. 1. Schematic depiction of TTL physical processes vs longitude and height.

We have a high level of confidence in the estimated accuracy of the DLH and NW measurements (≃5%–10%) for two reasons. 1) The NW and DLH data obtained in the 2013 and 2014 flights show a high degree of consistency and agreement for TTL H_2O values less than 10 ppmv (see Fig. 7). 2) In TTL cirrus with very high ice concentrations (in excess of 1 cm^{-3}), the relative humidity with respect to ice (RH_{ice}) is consistently near 100% (Jensen et al. 2013a). The time scale for quenching of supersaturation/subsaturation by ice crystal growth/sublimation in such clouds is a few minutes or less such that the RH_{ice} is expected to remain near 100%.

For the Guam ATTREX flights, TTL cirrus microphysical properties were measured with the SPEC Inc. Hawkeye instrument. Hawkeye is a combination of two imaging instruments [equivalent to the two-dimensional stereo (2D-S) probe (Lawson et al. 2006b) and the cloud particle imager (CPI; Lawson et al. 2001)], and a spectrometer [equivalent to the fast cloud droplet probe (FCDP; McFarquhar et al. 2007)], all of which have been used in the past for airborne cloud measurements. For consistency and

Fig. 2. The Global Hawk unmanned aircraft system. The wing pods, one with the Hawkeye instrument and the other with an aerodynamic/weight dummy for balance, are visible.

Table 1. Global Hawk payload. GSFC = Goddard Space Flight Center. JPL = Jet Propulsion Laboratory. CalTech = California Institute of Technology. UCLA = University of California, Los Angeles. LaRC = Langley Research Center. CIRES = Cooperative Institute for Research in Environmental Sciences. ESRL = Earth System Research Laboratory. CSD = Chemical Sciences Division. GMD = Global Monitoring Division. HFCs = hydrofluorocarbons. PFCs = perfluorocarbons.

Instrument	Investigator	Institution	Measurements
Remote			
CPL	M. McGill	NASA GSFC	Aerosol/cloud backscatter
MTP	M. Mahoney	JPL/Caltech	Temperature profile
DOAS	J. Stutz, K. Pfeilsticker	UCLA/University of Heidelberg	O_3, O_4, BrO, NO_2, OClO, IO H_2O, cloud properties
In situ			
DLH	G. Diskin	NASA LaRC	H_2O vapor
NW	T. Thornberry, A. Rollins	NOAA/CIRES	H_2O (vapor and total)
Hawkeye (2D-S, FCDP, CPI)	P. Lawson	SPEC, Inc.	Ice crystal size distributions, habits
NOAA Ozone (NW)	R.-S. Gao	NOAA/ESRL/CSD	O_3
HUPCRS	S. Wofsy	Harvard University	CO_2, CH_4, CO
UCATS	J. Elkins	NOAA/ESRL/GMD	N_2O, SF_6, CH_4, H_2, CO, O_3, H_2O
Solar and infrared radiometers	P. Pilewskie	University of Colorado Boulder	Zenith and nadir radiative fluxes
MMS	P. Bui	NASA ARC	Temperature, pressure, and winds
GWAS	E. Atlas	University of Miami	CFCs, halons, HCFCs, N_2O, CH_4, HFCs, PFCs, hydrocarbons, etc.

comparison with the 2011 and 2013 ATTREX flight series, a stand-alone FCDP was also included in the Guam payload. The combination of FCDP and 2D-S probes provides ice crystal size distributions spanning crystal maximum dimensions from about 1 μm to about 4 mm. The CPI provides detailed ice crystal images that can be used to determine habit information for crystals with maximum dimensions larger than about 40 μm. The cloud measurements, along with the water vapor and temperature measurements, are being used to test our theoretical understanding of ice crystal nucleation, depositional growth, and sedimentation (e.g., Jensen et al. 2013a; Ueyama et al. 2014, 2015).

The ATTREX payload included a number of tracer measurements that can be used to quantify TTL transport pathways and time scales. The Harvard University Picarro Cavity Ringdown System (HUPCRS) provides precise, stable measurements of CO_2 and CH_4. The HUPCRS also includes a CO channel that provides useful data with some averaging. The Unmanned Aircraft Systems (UAS) Chromatograph for Atmospheric Trace Species (UCATS) provides measurements of O_3, N_2O, SF_6, H_2, CO (tropospheric), and CH_4, as well as an additional measurement of water vapor.

The Global Hawk Whole Air Sampler (GWAS) provides 90 gas canister samples per flight. The times for the GWAS samples were determined on a real-time basis depending on the flight plan. Postflight, gas chromatographic analysis provides concentrations of a plethora of trace gases with sources from industrial midlatitude emissions, biomass burning, and the marine boundary layer, with certain compounds (e.g., organic nitrates) that have a unique source in the equatorial surface ocean. GWAS also measures a full suite of halocarbons that provide information on the role of short-lived halocarbons on chemistry in the tropical upper tropospheric–lower stratospheric (UTLS) region, on halogen budgets in the UTLS region, and on trends of hydrochlorofluorocarbons (HCFCs), chlorofluorocarbons (CFCs), and halogenated solvents.

The ATTREX payload also included radiation measurements, which will be used to quantify the impacts of clouds and water vapor variability on TTL radiative fluxes and heating rates. The spectral solar flux radiometer (SSFR) measurements additionally provide information about cirrus microphysical properties, and retrieval of TTL water vapor amounts with SSFR spectra has been demonstrated (Kindel et al. 2015). Last, the

miniature differential optical absorption spectroscopy (mini-DOAS) instrument provides measurements of BrO, NO_2, O_3, IO, O_4, H_2O, and cloud/aerosol extinction at various elevation angles near the limb. These measurements can be converted to vertical trace gas concentration profiles from 1 km above to 5 km below flight altitude using radiative transfer calculations and either optimal estimation or O_3 absorption techniques. The combination of the mini-DOAS BrO (and IO) measurements and GWAS measurements of major halogenated hydrocarbons provides constraints on the TTL and lower-stratospheric Br_y and I_y budgets.

Two additional remote sensing instruments were included that provide both valuable science data and real-time information for flight operations. The cloud physics lidar (CPL) provides profiles of aerosol/cloud backscatter and depolarization below the aircraft. The high sensitivity of CPL backscatter measurements have proven useful for detecting tenuous TTL cirrus (Davis et al. 2010), and the depolarization measurement provides information about ice crystal habits. The microwave temperature profiler (MTP) provides vertical profiles of temperature above and below the aircraft. The CPL and MTP data were transmitted to the Global Hawk ground operations center via a high-speed data link, and the information was used to determine when to execute vertical profiles through the TTL.

ATTREX 2014 GLOBAL HAWK FLIGHTS. The overall ATTREX project included multiple campaigns: flights were conducted out of AFRC in the fall of 2011 and the winter–spring of 2013 [see Jensen et al. (2013b) for details]. Here, we report on the 2014 deployment to Guam in the western Pacific during February and early March 2014. The flight paths for the six Guam Global Hawk flights are shown in Fig. 3, along with the earlier ATTREX flights for context. The Coordinated Airborne Studies in the Tropics (CAST) and the Convective Transport of Active Species in the Tropics (CONTRAST) campaigns were planned to be concurrent with the ATTREX Guam flights. The CAST and CONTRAST campaigns are described in separate articles in this issue. A series of aircraft operations problems delayed the Global Hawk flights until the CAST and CONTRAST operations were essentially completed. Nevertheless, the combined lower- to midtroposphere sampling from CAST and CONTRAST flights and upper tropospheric–lower stratospheric ATTREX Global Hawk measurements provide unique information about the western tropical Pacific atmospheric composition from the surface to the stratosphere.

The Guam flights provided an extensive survey of western Pacific TTL composition. Details of the individual Global Hawk flights from Guam are provided in Table 2. The general sampling strategy was to execute numerous vertical profiles between 45,000 ft (≃13.7 km) and cruise altitude [53,000–60,000 ft (≃16.2–18.3 km), depending on the fuel load]. Figure 4 shows the resulting coverage in longitude, latitude, and height space. Global Hawk power constraints forced us to turn off the GWAS pumps on descents; thus, GWAS samples were taken during the ascents only.

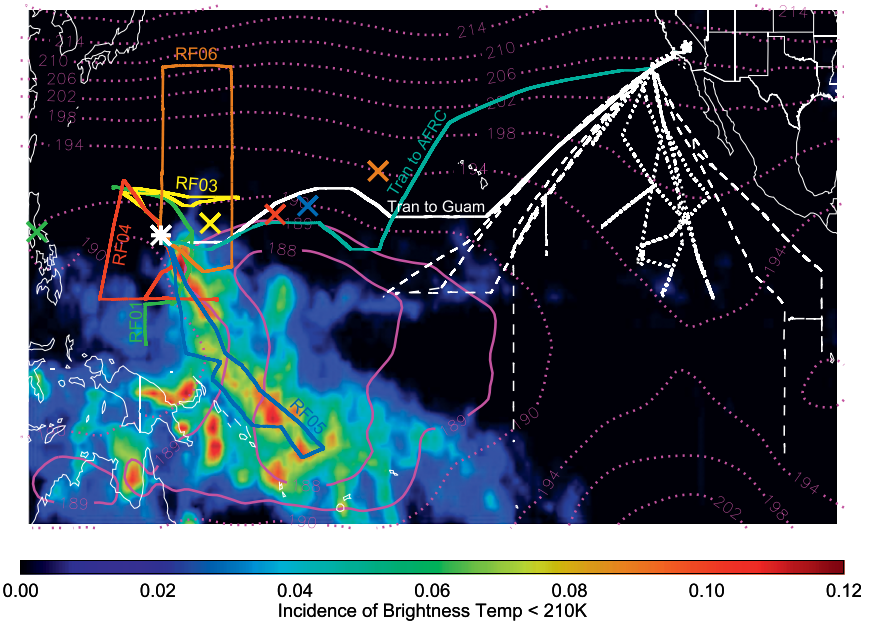

Fig. 3. Global Hawk Guam deployment flight paths. Note that for RF02, the aircraft simply profiled over Guam. The paths of the 2011 and 2013 ATTREX flights from AFRC in Southern California are shown (white lines) for context. Average 95-hPa temperatures for the 1 Feb–15 Mar period from ERA-Interim are overplotted, along with the incidence of infrared brightness temperatures less than 210 K (from geostationary meteorological satellites). In the tropics, 210 K is at 165 hPa, just below the mean altitude of deep convective cloud tops. The colored ×'s mark the approximate position of the Northern Hemisphere monsoon anticyclone discussed in the text for the corresponding research flights.

The transit from AFRC to Guam on 16–17 January 2014 served primarily to transport the Global Hawk to the deployment location. Concerns about fuel consumption and the limited ability to transmit commands to the aircraft payload during the flight precluded the execution of vertical profiles through the TTL. The aircraft cruised near the tropical tropopause for most of the flight. As mentioned above, aircraft operational and mechanical problems (as well as unusually severe local weather in Guam) prevented Global Hawk flights for the next several weeks after arrival in Guam while CONTRAST and CAST were underway.

The prevailing meteorological pattern in the boreal winter western Pacific TTL has a pool of cold temperatures located just east of the most active convection (Randel and Wu 2005; see Fig. 3). These cold temperatures are essentially a wave response to the convective heating and uplift; as part of this wave response, there is a boreal hemisphere anticyclone, usually centered north and slightly east of the cold temperature pool. There is frequently a corresponding anticyclone in the Southern Hemisphere, though this was typically out of range of ATTREX sampling. The convection (which is strongest in the Southern Hemisphere during boreal winter, though there is significant penetration to Northern Hemisphere latitudes; Fig. 3) is modulated by the Madden–Julian oscillation (MJO; Madden and Julian 1994). This oscillation produces substantial fluctuations in the position and intensity of the cold temperature pool and the associated anticyclone. The primary research flights occurred during the period 12 February through 13 March, during which time the cold pool and anticyclone basically moved from well west of Guam to the central Pacific, roughly consistent with the propagation of the MJO. The progression of the center of the anticyclone with the various research flights is shown by the "×" symbols in Fig. 3.

The first ATTREX local research flight (RF01) from Guam occurred on 12–13 February. The primary focus of this flight was to survey the composition, humidity, clouds, and thermal structure of the western Pacific TTL. During this flight, convection was most active well west of Guam and was suppressed at Guam's longitudes, so the center of monsoon anticyclone (Fig. 3) and the coldest TTL temperatures were also west of Guam. A semi-Lagrangian flight plan, approximately along the streamlines of the anticyclone, was chosen, arcing north and west of Guam, and then reversing course and heading south of Guam down to near the equator. Limitations on Global Hawk operations in cold temperatures and aerodynamic drag prevented the aircraft from climbing above about 57,000 ft (17.8 km). Cirrus clouds were observed throughout the TTL, almost certainly formed in situ because of the absence of nearby convection. Given the westward position of the anticyclone, the TTL circulation was from the west-northwest, and back trajectory analysis showed that a significant portion of the air sampled had progressed clockwise around the anticyclone after having been detrained from convective systems in Africa about a week to 10 days prior to the time of observation. The CO_2 and methane measurements were consistent with this picture.

The trajectory method used is similar to that described in Pfister et al. (2001) and Bergman et al. (2012); that is, diabatic back trajectories are calculated from clusters of points surrounding the aircraft measurements using European Centre for Medium-Range Weather Forecasts interim reanalyses (ERA-Interim) and calculated diabatic heating rates typical for the boreal winter season (Yang et al. 2010). These back trajectories are routed through 3-hourly fields of cloud-top potential temperature derived from global infrared brightness temperatures, global rainfall rates, and analysis temperatures. Convective influence is said to occur when an air parcel is over a convective system and its

Table 2. ATTREX Guam Global Hawk flights. UT = universal time.

Flight	Date in 2014	Takeoff time (UT), duration (h)	No. of profiles	Science foci
Transit to Guam	16–17 Jan	0416, 19.9	1	Transit aircraft to Guam
RF01	12–13 Feb	1747, 17.5	30	TTL survey, cirrus sampling
RF02	16–17 Feb	1718, 17.7	26	TTL survey, cirrus sampling
RF03	4–5 Mar	1728, 12.7	20	Tropical cyclone Faxai sampling, cirrus sampling
RF04	6–7 Mar	1700, 17	24	TTL survey, wave measurements
RF05	9–10 Mar	1524, 19.7	34	Southern survey, convective outflow
RF06	11–12 Mar	1653, 15.3	32	Northern/midlatitude survey
Transit to AFRC	13–14 Mar	1953, 19.4	31	Pacific tropical survey, cirrus sampling

potential temperature is lower than the cloud-top potential temperature. The method allows for calculation of both the time to the most recent convection for a given sampled air parcel and the location of that most recent convection, allowing air from African convection to be sampled, which was apparent in the CO_2 and methane measurements.

The second flight (RF02; 16–17 February) occurred as the monsoon anticyclone was reforming east of Guam. There was very active convection about 7° south of Guam, which undoubtedly contributed to the substantial change in the anticyclone's position. Shortly after takeoff on RF02, the primary satellite communications system for Global Hawk command and control (Inmarsat) was discovered to be inoperative. As a result, the aircraft was forced to stay within line of sight of the ground station on Guam. The aircraft circled in the zone next to Guam reserved for unmanned aircraft climb-out and final descent for 17.5 h, providing 26 vertical profiles through the TTL. This turned out to be an interesting location to profile on this day, with a distinct double-cold-point temperature structure and corresponding vertical lamination in tracer concentrations that is related to the wave motions (Thompson et al. 2011). TTL cirrus streaming over Guam from deep convection to the southeast were sampled much of the time on this flight. The stationary position of the aircraft over Guam allowed high-time-resolution sampling of an inertia–gravity wave with a peak-to-peak amplitude of about 5 K. This wave contributed to the in situ formation of observed TTL cirrus at the cold point near 17.7-km altitude. The CAST and CONTRAST aircraft [Natural Environment Research Council (NERC) BAe-146 and National Science Foundation (NSF) G-5] sampled near the Global Hawk flight path on this day.

For the remainder of February, convection continued to strengthen just south of Guam, consistent with the onset of the active phase of the MJO. In response, the upper-level anticyclone was pushed east of Guam, along with the coldest tropopause temperatures. As preparations for RF03 were underway around the beginning of March, a tropical cyclone was developing southeast of Guam. By the time of RF03 on 4–5 March, Tropical Cyclone Faxai had swept northward east of Guam and briefly reached typhoon status around the time the Global Hawk sampled the TTL in the vicinity of the storm (see Fig. 5). The flight path took the aircraft northwest from Guam and then along an eastbound leg just south of the cyclone. Multiple vertical profiles were executed through the outflow cirrus cloud emanating from the cyclone. Except for a few occasions at the highest altitudes, the observed flow was from the south and southwest, so the air sampled during multiple vertical profiles was about 0.5–2 days old, having detrained from the cyclone when it was actually south of the flight track. Temperatures were sufficiently cold (the coldest measured temperatures during the ATTREX Guam flights) to maintain (or reform) the outflow cirrus from the cyclone over that period of time. The TTL cirrus tops were as high as 17.3 km. The flight provides an excellent case study of TTL composition perturbation by deep, organized convection.

The tropical cyclone sampled by RF03 marked the beginning of a shift of convection toward the Southern Hemisphere, a weakening of the monsoon anticyclone, and a clear eastward propagation

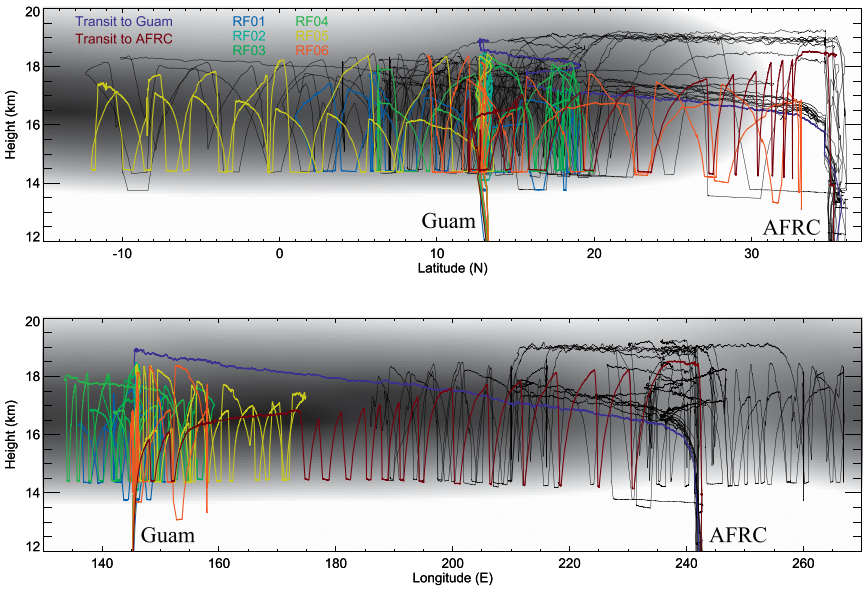

Fig. 4. Latitude, longitude, and height coverage of ATTREX Global Hawk flights. Black curves correspond to ATTREX1 (2011) and ATTREX2 (2013); colored curves show the ATTREX3 flights from Guam. The grayscale background shows the (top) mean temperature vs latitude and height at the Guam longitude and (bottom) temperature vs longitude and height at the Guam latitude. The darkest shading indicates mean temperatures approaching 188 K, and the lightest shading indicates mean temperatures greater than 205 K.

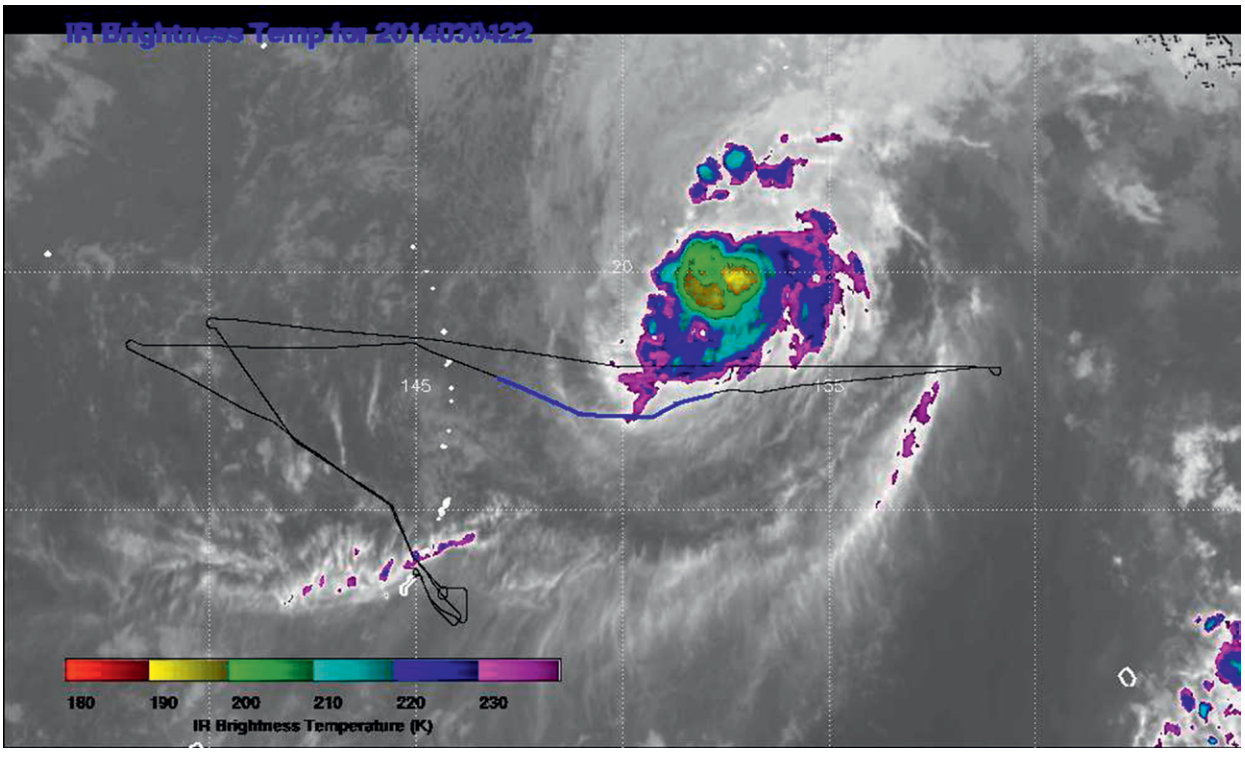

Fig. 5. RF03 flight path just south of Tropical Cyclone Faxai.

of the MJO. In response to the shift in convection, the coldest temperatures moved into the Southern Hemisphere. The 6–7 March (RF04) flight took place in this environment, providing an additional survey of western Pacific TTL tracers and cirrus. The aircraft was directed south to 6°N and then flew a long, approximately constant-altitude leg at this latitude where multiple radiosonde stations are located, with the objective of characterizing wave properties with the combination of MMS and MTP measurements and the radiosondes. Because of the weakening anticyclone and shift of cold temperatures and convection to the Southern Hemisphere, this flight had temperatures about 3 K warmer than typical of the other flights (the minimum temperature for RF04 was about 188 K). The amount of fresh (less than 2 days) convective injection was notably less than during RF03, though there was significant convective influence about 3–5 days old from the strong MJO that had dominated the last two weeks of February. Even though temperatures were warmer in RF04 than in the other flights, some of the highest thin cirrus (up to 17.9 km) were observed on this flight.

The fifth local flight (RF05) on 9–10 March served as a southern survey and included considerable sampling in the outflow of strong convection. The goal was to reach about 20°S, but the aircraft had to turn back near 12°S owing to a line of intense convection that developed at about 17°S, reaching the cold-point tropopause at about 17 km. Tropical Cyclone Lusi was developing at 15°S just east of the flight track. Cirrus with high ice water content and numerous ice crystals were sampled up to the cold-point tropopause along the southernmost leg of the flight. Prevailing winds at flight level were from the east and southeast, so this air mass originated from the line of convection to the south.

Flight RF06 on 11–12 March served as a northern survey and was confined to latitudes north of 10°N, with multiple vertical profiles on both the tropical and extratropical sides of the subtropical jet. Two of the profiles north of the jet extended down to 43,000 ft (≈13.1 km) in order to sample as much of the extratropical lowermost stratosphere as possible. The objective of this flight was to provide tracer measurements both in the TTL and in the extratropical lower stratosphere for quantification of the role of inmixing on TTL composition. As in the case for RF05, both convection and the coldest temperatures were south of the equator, so very little fresh convection was noted on this flight. A developing trough in the midlatitude western Pacific moved the boundary between midlatitude and tropical air southward, making the midlatitude air more accessible for sampling. Minimum temperatures were typically about 189 K in RF06, substantially warmer than the other flights.

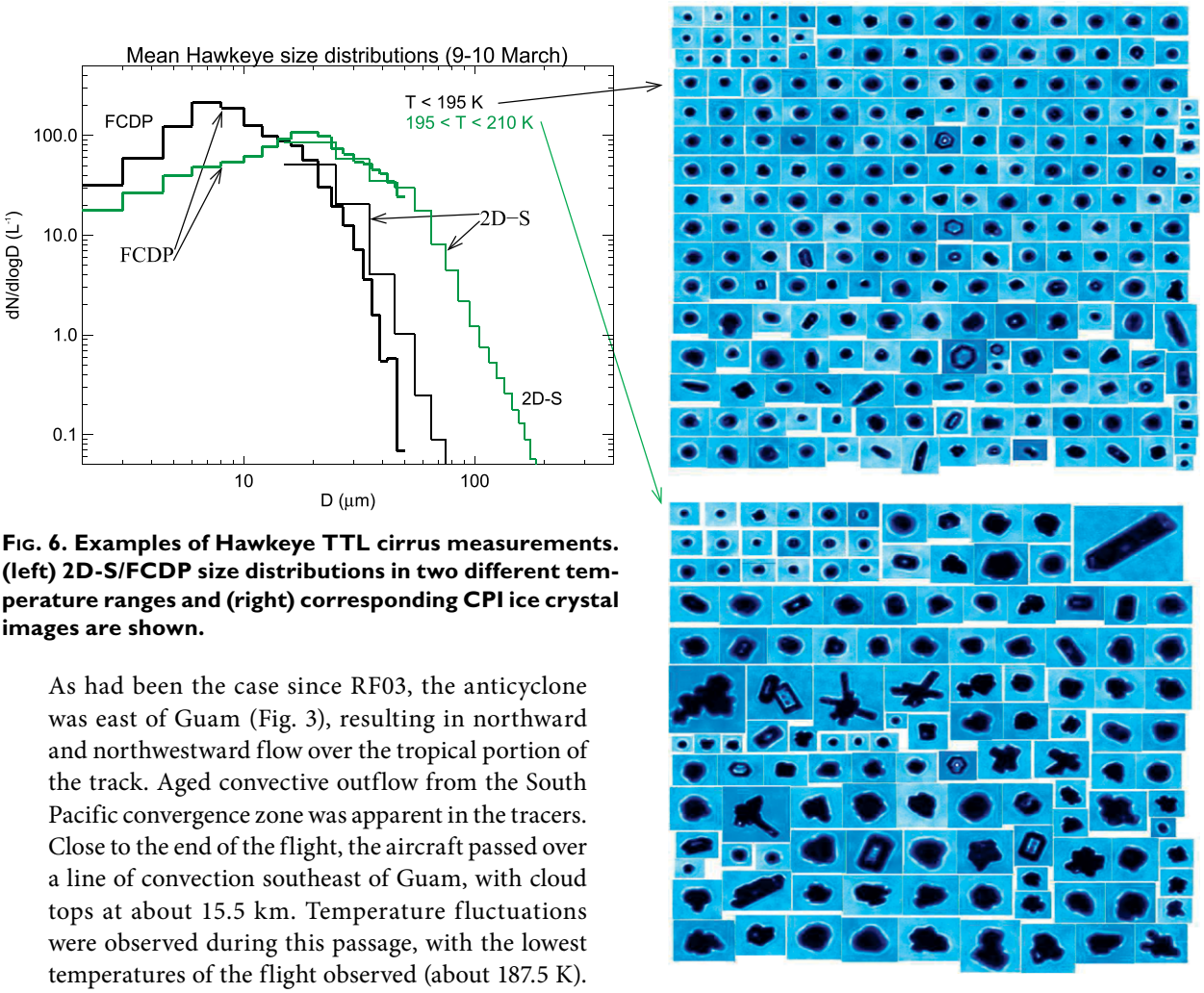

Fig. 6. Examples of Hawkeye TTL cirrus measurements. (left) 2D-S/FCDP size distributions in two different temperature ranges and (right) corresponding CPI ice crystal images are shown.

As had been the case since RF03, the anticyclone was east of Guam (Fig. 3), resulting in northward and northwestward flow over the tropical portion of the track. Aged convective outflow from the South Pacific convergence zone was apparent in the tracers. Close to the end of the flight, the aircraft passed over a line of convection southeast of Guam, with cloud tops at about 15.5 km. Temperature fluctuations were observed during this passage, with the lowest temperatures of the flight observed (about 187.5 K). The aircraft was able to descend downstream of this convection and sample the outflow.

The transit back to AFRC provided the first opportunity to perform vertical profiling in the central Pacific (since the transit from AFRC to Guam was entirely at cruise altitude). At this time convection was reforming north of the equator but consistent with the eastward propagation of the MJO; the convection was well east of Guam. In response to the increased Northern Hemisphere convection, cold temperatures in the TTL moved north and occupied a large area centered on the equator and east of the convection (and east of the date line). For the most part, the gradual climb to 17 km during the first 6 h of the flight was in relatively warm temperatures and downstream of a large, deep convective system with cloud tops up to the cold-point tropopause. During this portion of the flight, a layer of ice crystals and freshly lofted air (age about a day) was observed, with minimum temperatures of ≃192 K. About 6 h into the flight, as the aircraft crossed the date line, vertical profiling in the cold pool commenced. Temperatures were 5 K colder east of the date line, the air was considerably older (3 days to a week, depending on altitude, with the older air at higher altitudes), and substantial cirrus were observed. The transit back to AFRC provided an additional survey of TTL composition across the western and central Pacific.

OVERVIEW OF ATTREX MEASUREMENTS. It was recognized in the ATTREX planning stage that the boreal wintertime western Pacific is a region with very high occurrence frequency of clouds in the TTL (Wang et al. 1996), and the ATTREX Guam flights provided a wealth of TTL cirrus measurements. As indicated by the Hawkeye measurements, the Global Hawk was inside TTL cirrus more than 34 h during the flights from Guam. Figure 6 shows examples of ice crystal images and size distributions provided by Hawkeye. The CPI images often indicated bullet rosette habits and a lack of evidence for ice crystal aggregates even on flight segments in cirrus that appeared to be associated with deep convection. The

existence of bullet rosettes is generally an indication of in situ nucleation and growth of ice crystals, whereas aggregates are typically observed in fresh anvil cirrus (Lawson et al. 2006a). The ATTREX data support earlier results indicating that in situ nucleation and/or deposition growth of anvil ice crystals are important processes for generating and maintaining extensive cirrus shields around tropical deep convection (Whiteway et al. 2004).

As discussed above, the ATTREX DLH and NOAA water vapor (NWV) instruments provided precise water vapor measurements. Figure 7 shows frequency distributions of TTL relative humidity with respect to ice from the Guam flights and a comparison between DLH and NWV. The strong peak near RH_{ice} = 100% is expected since vapor deposition on and sublimation from cirrus ice crystals will tend to drive the water vapor concentration toward ice saturation. Consistent with ice nucleation and growth theory, substantial supersaturations with respect to ice occur frequently in the TTL (Jensen et al. 2001). The observations of large ice supersaturations indicate that the dehydration of air passing through the TTL is less efficient than currently assumed in global models, and that the model representations of TTL cirrus processes need to be modified to include supersaturation both in clear-sky regions and within cirrus. The agreement between relative humidities indicated by DLH and NWV is excellent, even at the very low mixing ratios encountered during the ATTREX flights.

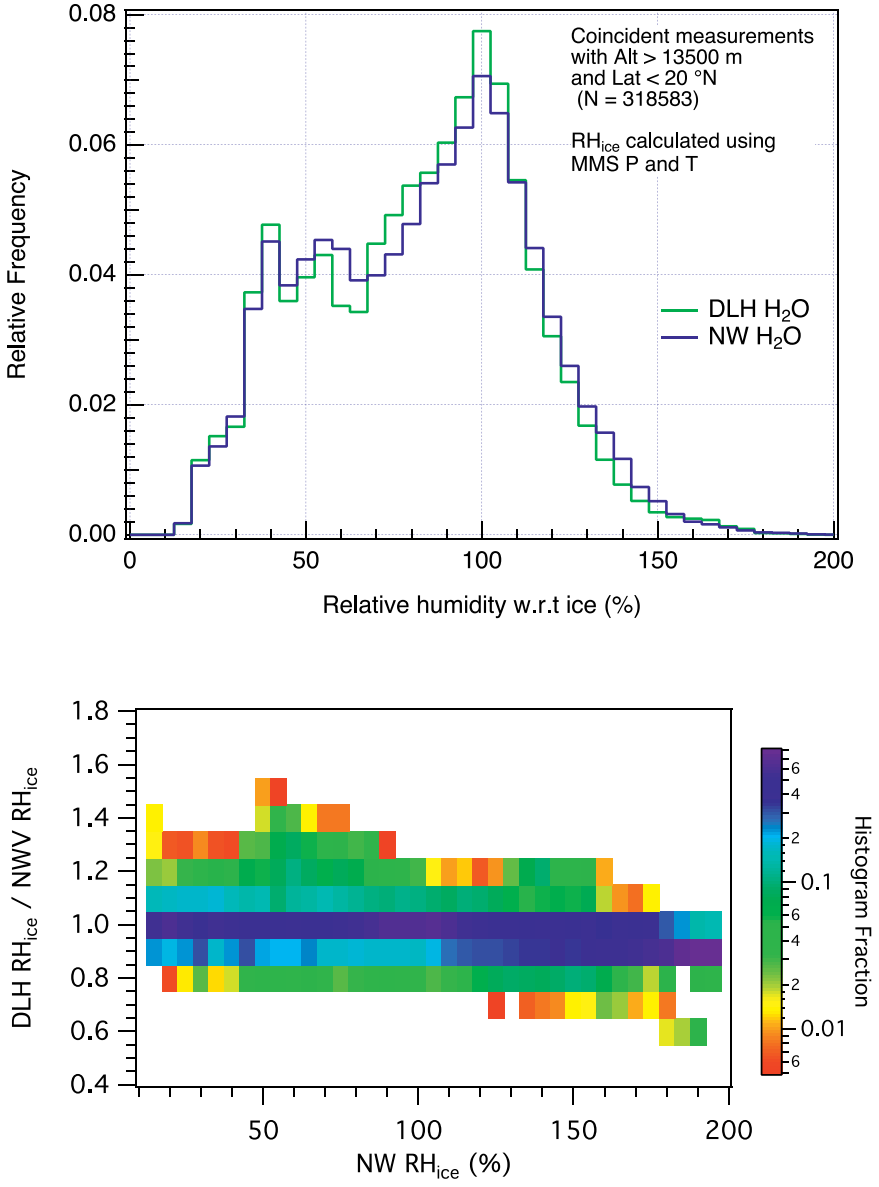

Fig. 7. (top) Frequency distributions of western Pacific TTL relative humidity with respect to ice from DLH (green) and NWV (blue). Both datasets indicate a peak near 100% corresponding to data inside cirrus and the common occurrence of supersaturation with respect to ice. (bottom) Ratio of DLH to NWV relative humidity with respect to ice vs the NWV relative humidity.

One of the objectives of ATTREX was to investigate how waves affect the TTL cirrus formation and dehydration processes. RF04 flight was designed to survey horizontal wave structures and cirrus–wave relationships. An overflight at cruise altitudes of 17.5–18 km along 134°–153°E at the nearly constant latitude of 6°N provided continuous vertical scans of clouds by the onboard down-looking CPL, as shown in Fig. 8. Although ice particles were not detected at the flight altitudes in this segment due to warmer temperatures than other flights (or upstream regions), the CPL was able to observe a zonally varying, extensive cirrus layer below flight level. The cloud layer at ≃12–16 km appears to be associated with a 10-day Kelvin wave

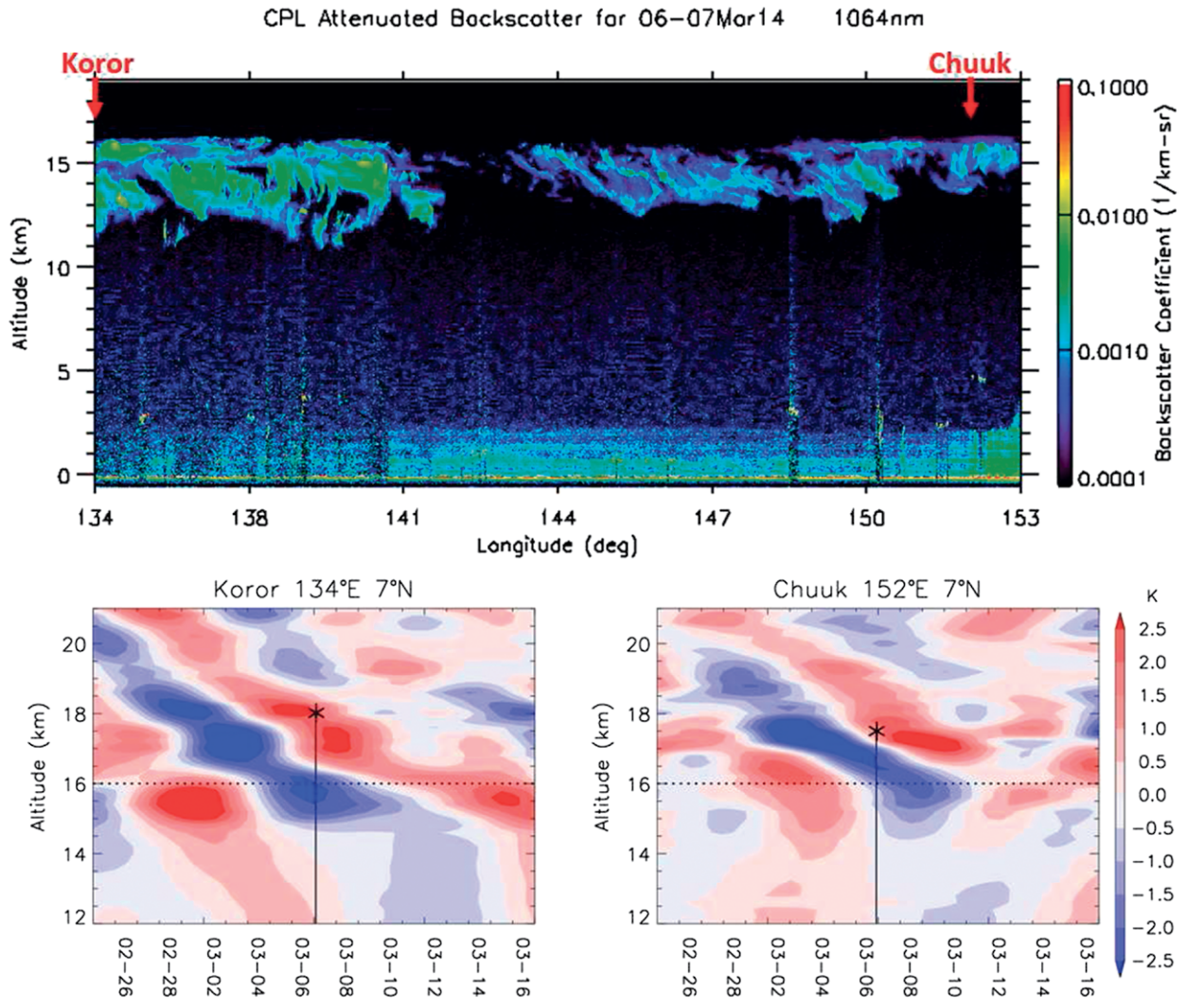

Fig. 8. (top) CPL clouds from the cruise altitude flight segment along 134°–153°E at 6°N in RF04. Arrows indicate the nearby locations of radiosondes (Koror and Chuuk). (bottom left) Radiosonde temperature anomalies filtered with 7–15-day periods for Koror. The asterisk shows the aircraft position, and the thin vertical line is the view of the CPL. The dashed line indicates the top of the cirrus layer at about 16 km, which is approximately collocated with the cold-point tropopause. (bottom right) As in (bottom left), but for Chuuk.

that was identified by spectral analysis of radiosonde data at Koror, Republic of Palau (7°N, 134°E), and Chuuk, Federated States of Micronesia (7°N, 152°E). The bottom two panels of Fig. 8 show 7–15-day filtered temperature anomalies at the two radiosonde sites. Koror was near the coldest phase of the Kelvin wave and Chuuk was near the beginning of the cold phase on 6–7 March, suggesting that the wave had about a zonal wavenumber of 5 (≃8,000-km wavelength) with its peak near Koror and node near Chuuk. The change in the Kelvin wave amplitude likely induced the change from a thicker persistent cloud layer in the west to a thinner broken cloud layer in the east.

Figure 9 shows an example of tracers measured in the vicinity of Typhoon Faxai on RF03. The CO_2 and CH_4 concentrations between 350- and 370-K potential temperatures measured on this flight (colored data points) were the highest values encountered over the tropical western Pacific. We examined surface measurements at various NOAA stations over the tropical Pacific in order to compare chemical signatures at the surface and the fresh, convectively lofted air. We find that concentrations of both CO_2 and CH_4 from Mauna Loa, Hawaii, agree well with the extreme concentrations sampled by the aircraft on this flight, suggesting rapid injection of nearby air from the tropical Northern Hemisphere and little contribution from the tropical Southern Hemisphere. Also shown in Fig. 9 are CO_2 concentrations sampled at other geographical locations and times during the ATTREX

flights from Guam (gray data points). The spread in CO_2 concentrations below 370 K reflects inputs from both the Northern and Southern Hemispheres. Above 370 K, we find reduced variability in CO_2 and a profile shape dictated by the phase of the CO_2 seasonal cycle—namely, the gradual build up as the biosphere transitions from photosynthesis to respiration—ascending throughout the TTL over time.

Numerous trace gases were measured by the whole air sampler to better define the composition and variation of organic compounds in the TTL region. ATTREX measurements expanded by over an order of magnitude the available data of organic chemical composition in the TTL region. The gases that were measured included a range of C_2–C_4 nonmethane hydrocarbons, long-lived chlorofluorocarbons and hydrochlorofluorocarbons, various halogenated solvents, selected organic sulfur and nitrogen species, and a full range of halogenated methanes. Compounds of different lifetimes and source emission regions are being used to evaluate mixing, transport, and chemistry in the TTL region. A high priority for the ATTREX mission was to define the input of reactive bromine to the stratosphere from both short-lived species [such as bromoform ($CHBr_3$)], as well as the longer-lived compounds (such as halons and methyl bromide). These measurements (along with ozone) are illustrated in Fig. 10. The average concentration of short-lived brominated compounds contributes approximately 18% of the total organic bromine at the tropical tropopause. The data will be used in conjunction with the BrO measurements from the DOAS instrument to examine the total bromine budget and partitioning between organic and inorganic bromine in the TTL and lower stratosphere.

SUMMARY AND DISCUSSION. The 2014 ATTREX deployment to Guam has provided a unique dataset of highly resolved tracer, cloud, water vapor, chemical radical, and radiation measurements in the western Pacific tropical tropopause layer. The wintertime western Pacific TTL is particularly important for controlling stratospheric composition because the coldest tropopause temperatures and strongest vertical ascent rates occur in this region. The six Global Hawk flights from Guam provided surveys of western Pacific TTL composition, measurements in regions recently influenced by deep convection, extensive sampling of TTL cirrus and relative humidity, spectrally resolved radiative flux measurements, measurements of TTL wave characteristics, and measurements of tracer gradients between the TTL and extratropical lower stratosphere.

The ATTREX measurements are being used for two general types of analyses: 1) phenomenological studies focused on understanding particular physical processes such as TTL transport pathways and rates, ice cloud formation and dehydration, dynamics controlling TTL thermal structure, and

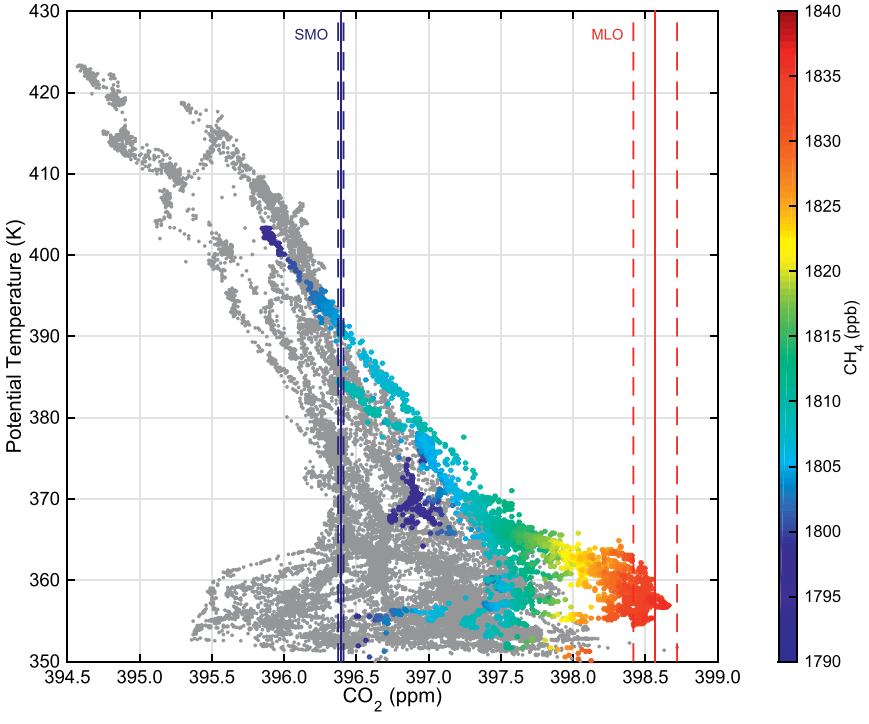

Fig. 9. Vertical profiles of CO_2 as a function of potential temperature for the tropical western Pacific (15°N–12°S) during all ATTREX flights from Guam (gray points). Highlighted in color are data from the flight south of the core of Typhoon Faxai on 4 Mar 2014 (RF03). The color corresponds to CH_4 concentrations at a given CO_2 concentration. Also shown are 11-day averages (solid lines) and minima and maxima (dashed lines) of CO_2 and CH_4 (color) concentrations at NOAA tropical surface stations in the Northern Hemisphere (Mauna Loa) and the Southern Hemisphere (American Samoa). The 11-day period extends from 27 Feb to 9 Mar 2014, which corresponds to the lifetime of the typhoon.

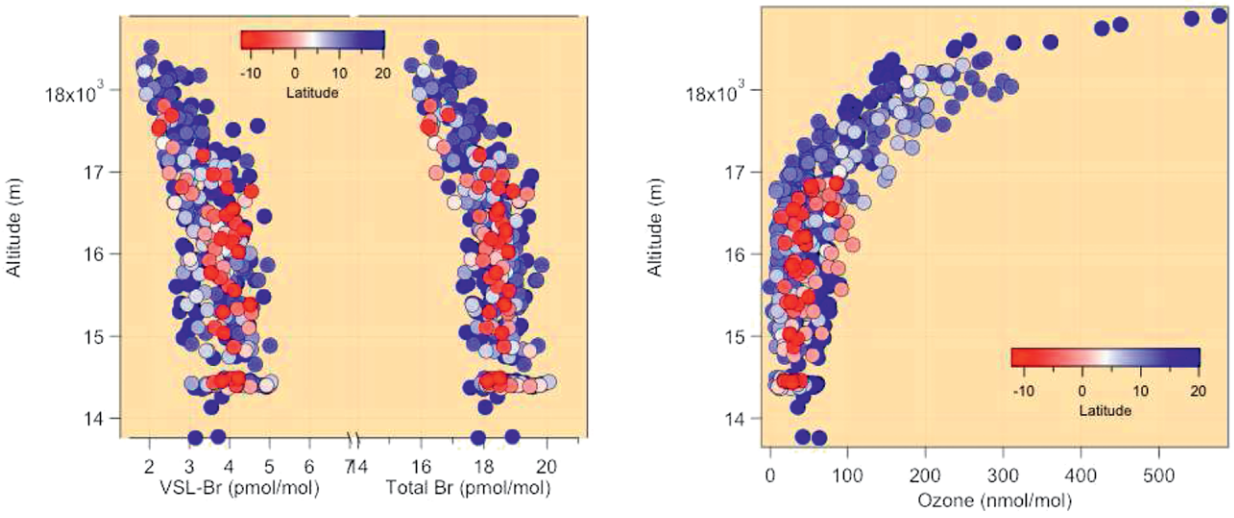

Fig. 10. Vertical profiles of selected trace gases measured in the TTL during the ATTREX Guam flights. (left) The GWAS data, including a full suite of organic bromine compounds, are shown. The very short-lived organic bromine (VSL-Br) species include $CHBr_3$, CH_2Br_2, CH_2BrCl, $CHBr_2Cl$, and $CHBrCl_2$. Total organic bromine (total Br) includes the VSL-Br species plus halons and CH_3Br. The very short-lived organic bromine compounds contributed approximately 18% to the total organic bromine at the tropical tropopause. No systematic influence of latitude was detected in the vertical gradients. (right) Ozone (nmol mol^{-1}) data from the UCATS instrument. Individual points are averaged over the sample integration time of the whole air samples. Ozone profiles tend to be anticorrelated with organic bromine concentrations in the TTL.

transport and chemical processes controlling halogen species concentrations; and 2) evaluation and improvement of global-model representations of these TTL processes. The precise, high-resolution tracer measurements in the remote western Pacific provided a wealth of information about both deep convective and large-scale transport into and through the TTL. The ATTREX measurement suite included tracers with maritime, industrial, biomass-burning, and Southern Hemisphere sources. The unprecedented accuracy and precision of the water vapor measurements permits quantitative investigations of cloud processes such as ice nucleation, crystal growth, sedimentation, and removal of vapor in excess of saturation. The long Global Hawk flights along with the high occurrence frequency of cirrus in the western Pacific TTL resulted in accumulation of about 34 h of sampling in clouds. This extensive dataset permits statistical analyses of the cloud properties and humidity in addition to studies of particular cloud events.

The ATTREX data are publicly available (https://espoarchive.nasa.gov/). However, data users are strongly encouraged to discuss the uncertainties and applicability of the measurements with the instrument leads listed in Table 1. Also, if the measurements are an important component of a scientific study, then coauthorship should be offered to the instrument investigators.

Numerous modeling and data analysis activities based on the ATTREX data are currently underway. The measurements are being used both for case-study process studies, such as understanding the processes leading to observed clouds and water vapor concentrations in particular regions (e.g., Ueyama et al. 2014; Evan et al. 2015), and for statistical comparison with models. The dataset is proving beneficial for evaluation of global-model representations of transport, chemical processes, and cloud processes. The combined datasets from CAST (lower–midtroposphere), CONTRAST (middle–upper troposphere), and ATTREX (upper–lower stratosphere) are being used to understand processes controlling short-lived organic and inorganic halogen species. The expectation is that the model improvements based on these analyses will improve the accuracy of climate predictions.

Although the ATTREX measurements have provided an invaluable dataset for studying TTL physical processes, a number of key measurement needs remain. Operational limits prevented the Global Hawk from sampling regions with temperatures colder than about 186 K. Trajectory calculations indicate that most air parcels transiting through the TTL during boreal wintertime experience colder temperatures. Measurements of water vapor and cloud properties at the lowest TTL temperatures would be useful for investigating dehydration processes at the point of minimum saturation

mixing ratio. The ATTREX payload did not include aerosol measurements, and very little information about TTL aerosol composition and physical properties is available. In particular, direct measurements of ice nuclei concentration and composition in the TTL are needed to definitively determine the relative importance of homogeneous and heterogeneous ice nucleation for production of TTL cirrus ice crystals.

The lack of suitable Global Hawk bases and cost issues prevented the originally planned ATTREX operations in the Southeast Asia region during boreal summertime. Physical processes controlling TTL humidity, clouds, and general composition are likely very different during the summertime "warm phase" of the tropical tropopause seasonal temperature variation. In particular, the summertime TTL and lower-stratosphere composition appears to be dominated by convection and radiative heating associated with the Asian monsoon (e.g., Rosenlof et al. 1997; Dethof et al. 1999; Fueglistaler et al. 2005). Aircraft measurements of TTL properties and physical processes in Southeast Asia during boreal summertime would help address these issues.

ACKNOWLEDGMENTS. We thank the Global Hawk project managers, pilots, and crew. Without their hard work overcoming numerous challenges, collection of the excellent data described here would not have been possible. Additional funding from the Deutsche Forschungsgemeinschaft (DFG) Grant PF 384 12/1 in support of the DOAS measurements and data processing is acknowledged.

REFERENCES

Bergman, J. W., E. J. Jensen, L. Pfister, and Q. Wang, 2012: Seasonal differences of vertical-transport efficiency in the tropical tropopause layer: On the interplay between tropical deep convection, large-scale vertical ascent, and horizontal circulations. *J. Geophys. Res.*, **117**, D05302, doi:10.1029/2011JD016992.

Davis, S. M., and Coauthors, 2010: In situ and lidar observations of tropopause subvisible cirrus clouds during TC4. *J. Geophys. Res.*, **115**, D00J17, doi:10.1029/2009JD013093.

Dethof, A., A. O'Neill, J. M. Slingo, and H. G. J. Smit, 1999: A mechanism for moistening the lower stratosphere involving the Asian summer monsoon. *Quart. J. Roy. Meteor. Soc.*, **125**, 1079–1106, doi:10.1002/qj.1999.49712555602.

Evan, S., K. H. Rosenlof, T. Thornberry, A. Rollins, and S. Khaykin, 2015: TTL cooling and drying during the January 2013 stratospheric sudden warming. *Quart. J. Roy. Meteor. Soc.*, **141**, 3030–3039, doi:10.1002/qj.2587.

Forster, P. M. F., and K. P. Shine, 2002: Assessing the climate impact of trends in stratospheric water vapor. *Geophys. Res. Lett.*, **29**, doi:10.1029/2001GL013909.

Fueglistaler, S., M. Bonazzola, P. H. Haynes, and T. Peter, 2005: Stratospheric water vapor predicted from the Lagrangian temperature history of air entering the stratosphere in the tropics. *J. Geophys. Res.*, **110**, D08107, doi:10.1029/2004JD005516.

——, A. E. Dessler, T. J. Dunkerton, I. Folkins, Q. Fu, and P. W. Mote, 2009: The tropical tropopause layer. *Rev. Geophys.*, **47**, RG1004, doi:10.1029/2008RG000267.

Jensen, E. J., L. Pfister, A. S. Ackerman, A. Tabazadeh, and O. B. Toon, 2001: A conceptual model of the dehydration of air due to freeze-drying by optically thin, laminar cirrus rising slowly across the tropical tropopause. *J. Geophys. Res.*, **106**, 17 273–17 252, doi:10.1029/2000JD900649.

——, and Coauthors, 2013a: Ice nucleation and dehydration in the Tropical Tropopause Layer. *Proc. Natl. Acad. Sci. USA*, **110**, 2041–2046, doi:10.1073/pnas.1217104110.

——, and Coauthors, 2013b: The NASA Airborne Tropical TRopopause EXperiment (ATTREX). *SPARC Newsletter*, No. 41, SPARC International Project Office, Zurich, Switzerland, 15–24.

Kindel, B. C., P. Pilewskie, K. S. Schmidt, T. Thornberry, A. Rollins, and T. Bui, 2015: Upper-troposphere and lower-stratosphere water vapor retrievals from the 1400 and 1900 nm water vapor bands. *Atmos. Meas. Tech.*, **8**, 1147–1156, doi:10.5194/amt-8-1147-2015.

Lawson, R. P., B. A. Baker, C. G. Schmitt, and T. L. Jensen, 2001: An overview of microphysical properties of Arctic clouds observed in May and July during FIRE ACE. *J. Geophys. Res.*, **106**, 14 989–15 014, doi:10.1029/2000JD900789.

——, ——, B. Pilson, and Q. Mo, 2006a: In situ observations of the microphysical properties of wave, cirrus and anvil clouds. Part II: Cirrus clouds. *J. Atmos. Sci.*, **63**, 3186–3203, doi:10.1175/JAS3803.1.

——, D. O'Connor, P. Zmarzly, K. Weaver, B. A. Baker, Q. Mo, and H. Jonsson, 2006b: The 2D-S (stereo) probe: Design and preliminary tests of a new airborne, high-speed, high-resolution imaging probe. *J. Atmos. Oceanic Technol.*, **23**, 1462–1477, doi:10.1175/JTECH1927.1.

Madden, R. A., and P. R. Julian, 1994: Observations of the 40–50-day tropical—A review. *Mon. Wea. Rev.*, **122**, 814–837, doi:10.1175/1520-0493(1994)122<0814:OOTDTO>2.0.CO;2.

McFarquhar, G. M., J. Um, M. Freer, D. Baumgardner, G. L. Kok, and G. Mace, 2007: The importance of small ice crystals to cirrus properties: Observations from the Tropical Warm Pool International Cloud

Experiment (TWP-ICE). *Geophys. Res. Lett.*, **34**, L13803, doi:10.1029/2007GL029865.

Oltmans, S. J., and K. H. Rosenlof, 2000: Data quality. SPARC assessment of upper tropospheric and stratospheric water vapour, D. Kley, J. M. Russell III, and C. Phillips, Eds., World Climate Research Programme 113, WMO Tech. Doc. WMO/TD-1043, SPARC Rep. 2, 312 pp.

Pfister, L., and Coauthors, 2001: Aircraft observations of thin cirrus clouds near the tropical tropopause. *J. Geophys. Res.*, **106**, 9765–9786, doi:10.1029/2000JD900648.

Randel, W. J., and F. Wu, 2005: Kelvin wave variability near the equatorial tropopause observed in GPS radio occultation measurements. *J. Geophys. Res.*, **110**, D03102, doi:10.1029/2004JD005006.

Rosenlof, K. H., A. F. Tuck, K. K. Kelly, J. M. Russell, and M. P. McCormick, 1997: Hemispheric asymmetries in water vapor and inferences about transport in the lower stratosphere. *J. Geophys. Res.*, **102**, 13 213–13 234, doi:10.1029/97JD00873.

Solomon, S., K. Rosenlof, R. Portmann, J. Daniel, S. Davis, T. Sanford, and G.-K. Plattner, 2010: Contributions of stratospheric water vapor changes to decadal variations in the rate of global warming. *Science*, **327**, 1219–1223, doi:10.1126/science.1182488.

Thompson, A. M., A. L. Allen, S. Lee, S. K. Miller, and J. C. Witte, 2011: Gravity and Rossby wave signatures in the tropical troposphere and lower stratosphere based on Southern Hemisphere Additional Ozonesondes (SHADOZ), 1998–2007. *J. Geophys. Res.*, **116**, D05302, doi:10.1029/2009JD013429.

Thornberry, T. D., A. W. Rollins, R. S. Gao, L. A. Watts, S. J. Ciciora, R. J. McLaughlin, and D. W. Fahey, 2015: A two-channel, tunable diode laser-based hygrometer for measurement of water vapor and cirrus cloud ice water content in the upper troposphere and lower stratosphere. *Atmos. Meas. Tech.*, **8**, 211–244, doi:10.5194/amt-8-211-2015.

Ueyama, R., L. Pfister, E. J. Jensen, G. S. Diskin, T. P. Bui, and J. M. Dean-Day, 2014: Dehydration in the tropical tropopause layer: A case study for model evaluation using aircraft observations. *J. Geophys. Res. Atmos.*, **119**, 5299–5316, doi:10.1002/2013JD021381.

——, E. J. Jensen, L. Pfister, and J.-E. Kim, 2015: Dynamical, convective, and microphysical control on wintertime distributions of water vapor and clouds in the tropical tropopause layer. *J. Geophys. Res. Atmos.*, **120**, 10 483–10 500, doi:10.1002/2015JD023318.

Wang, P.-H., P. Minnis, M. P. McCormick, G. S. Kent, and K. M. Skeens, 1996: A 6-year climatology of cloud occurrence frequency from Stratospheric Aerosol and Gas Experiment II observations (1985–1990). *J. Geophys. Res.*, **101**, 29 407–29 429, doi:10.1029/96JD01780.

Weinstock, E. M., and Coauthors, 2009: Validation of the Harvard Lyman-α in situ water vapor instrument: Implications for the mechanisms that control stratospheric water vapor. *J. Geophys. Res.*, **114**, D23301, doi:10.1029/2009JD012427.

Whiteway, J., and Coauthors, 2004: Anatomy of cirrus clouds: Results from the Emerald airborne campaign. *Geophys. Res. Lett.*, **31**, L24102, doi:10.1029/2004GL021201.

Yang, Q., Q. Fu, and Y. Hu, 2010: Radiative impacts of clouds in the tropical tropopause layer. *J. Geophys. Res.*, **115**, D00H12, doi:10.1029/2009JD012393.